scientific reports

OPEN

Identification of epigenetic memory candidates associated with gestational age at birth through analysis of methylome and transcriptional data

Kohei Kashima[1,2,14]✉, Tomoko Kawai[2,14], Riki Nishimura[1], Yuh Shiwa[3], Kevin Y. Urayama[4,5], Hiromi Kamura[2], Kazue Takeda[6], Saki Aoto[7], Atsushi Ito[1], Keiko Matsubara[8], Takeshi Nagamatsu[9], Tomoyuki Fujii[9], Isaku Omori[10], Mitsumasa Shimizu[10], Hironobu Hyodo[11], Koji Kugu[11], Kenji Matsumoto[6], Atsushi Shimizu[3,12], Akira Oka[1], Masashi Mizuguchi[13], Kazuhiko Nakabayashi[2], Kenichiro Hata[2] & Naoto Takahashi[1]

Preterm birth is known to be associated with chronic disease risk in adulthood whereby epigenetic memory may play a mechanistic role in disease susceptibility. Gestational age (GA) is the most important prognostic factor for preterm infants, and numerous DNA methylation alterations associated with GA have been revealed by epigenome-wide association studies. However, in human preterm infants, whether the methylation changes relate to transcription in the fetal state and persist after birth remains to be elucidated. Here, we identified 461 transcripts associated with GA (range 23–41 weeks) and 2093 candidate CpG sites for GA-involved epigenetic memory through analysis of methylome (110 cord blood and 47 postnatal blood) and transcriptional data (55 cord blood). Moreover, we discovered the trends of chromatin state, such as polycomb-binding, among these candidate sites. Fifty-four memory candidate sites showed correlation between methylation and transcription, and the representative corresponding gene was *UCN*, which encodes urocortin.

Gestational age (GA) and birth weight, particularly low birth weight, are the most important predictors associated with short- and long-term neonatal adverse outcomes. Low birth weight infants can be classified as either preterm infants or small-for-gestational-age (SGA) infants. Preterm infants are defined as those born before 37 weeks of gestation. They are forced to survive *ex utero* midst their fetal development, receiving no direct nutrient and oxygen supply from their mothers, earlier than term infants. In contrast, SGA infants tend to be exposed to hypoxia and malnutrition in utero. Despite differences in etiology and exposure between these two conditions of newborns, both involve disturbed oxygen and nutrition during the perinatal period. To date, there is growing epidemiological evidence that these newborns may be at higher risk of chronic diseases in later

[1]Department of Pediatrics, The University of Tokyo Hospital, Hongo, Bunkyo-ku, Tokyo 113-8655, Japan. [2]Department of Maternal-Fetal Biology, National Research Institute for Child Health and Development, Tokyo, Japan. [3]Division of Biomedical Information Analysis, Iwate Tohoku Medical Megabank Organization, Disaster Reconstruction Center, Iwate Medical University, Iwate, Japan. [4]Department of Social Medicine, National Research Institute for Child Health and Development, Tokyo, Japan. [5]Graduate School of Public Health, St. Luke's International University, Tokyo, Japan. [6]Department of Allergy and Clinical Immunology, National Research Institute for Child Health and Development, Tokyo, Japan. [7]Medical Genome Center, National Research Institute for Child Health and Development, Tokyo, Japan. [8]Department of Molecular Endocrinology, National Research Institute for Child Health and Development, Tokyo, Japan. [9]Department of Obstetrics and Gynecology, The University of Tokyo Hospital, Tokyo, Japan. [10]Department of Neonatology, Tokyo Metropolitan Bokutoh Hospital, Tokyo, Japan. [11]Department of Obstetrics and Gynecology, Tokyo Metropolitan Bokutoh Hospital, Tokyo, Japan. [12]Division of Biomedical Information Analysis, Institute for Biomedical Sciences, Iwate Medical University, Iwate, Japan. [13]Department of Developmental Medical Sciences, The University of Tokyo, Tokyo, Japan. [14]These authors contributed equally: Kohei Kashima and Tomoko Kawai. ✉email: KASHIMAK-PED@h.u-tokyo.ac.jp

life, including coronary heart disease, type 2 diabetes, metabolic syndromes, and neurobehavioral problems[1–3]; higher risk of mortality from coronary heart disease has also been reported[2]. In addition, preterm and/or low birth weight infants are prone to metabolic shift including BMI gain[4], lower insulin sensitivity[5], and higher blood pressure[6]compared to normal birth weight infants, even in later childhood. Another line of evidence from the Dutch famine birth cohort studies showed that maternal undernutrition during pregnancy caused high morbidity of offspring in adulthood[7–9]. These findings support the Developmental Origins of Health and Disease (DOHaD) hypothesis[10,11] which describes that the adaptation for surviving harsh environment in early life may influence the susceptibility to chronic diseases in adulthood[10,11]. In other words, restriction of developmental plasticity may contribute to these personal traits[12]. Considering that epigenetic mechanisms play important roles in tissue differentiation and developmental plasticity[11,12], epigenetic memory formed in early development may therefore act upon pathways to chronic diseases in later life. However, this hypothesis has not been well-elucidated in humans.

Owing to advances in microarray technology, epigenome-wide association studies (EWAS) are now commonly conducted. In the perinatal field, previous studies have investigated methylation alterations related to GA[13–17], birth weight[15,18], and birth weight standard deviation (SD) scores for GA[19] by using cord blood samples. However, these studies have not examined whether DNA methylation changes relate to RNA expression levels, and those that were able to examine postnatal blood methylation showed inconsistent results. Two previous studies reported that certain methylation changes identified at birth among preterm or low birth weight infants were no longer observed by adulthood[15,20]; however, the results of postnatal methylation persistence were inconsistent[15,20]. Cruickschank et al. suggested that some methylation alterations among preterm infants may persist into adulthood[20]. In contrast, no persistence was observed from the age of 7 years in the report by Simkin et al. in the ARIES cohort study[15].

The objectives of the current study were to investigate epigenetic alterations associated with preterm birth and SGA through DNA methylation and gene expression microarrays, as well as, to identify epigenetic at-birth changes which may persist as personal traits after birth. The evaluation of DNA methylation, gene expression, and their relationship was performed using both genomic DNA and total RNA samples purified simultaneously. This is the first EWAS study targeting Japanese preterm and/or SGA infants.

Results

We generated normalized DNA methylation data from 110 cord blood samples and 47 postnatal peripheral blood samples, as well as, normalized gene expression data from 55 cord blood samples as described in Methods, Supplementary Methods, and Supplementary Figures 1–4. The results are described in the order shown in 'overall analysis framework' (Supplementary Figure 5). Among the 110 mother-infant pairs included in these analyses, mean GA was 34.0 weeks and mean birth weight SD score was − 0.6 (Table 1, Supplementary Table 1); 34.5% (n = 38) were small-for-GA (SGA; defined as birth weight < 10th percentile, equivalent to − 1.28 SD) and 10.9% (n = 12) were large-for-GA (LGA; defined as birth weight > 90th percentile, equivalent to 1.28 SD). Approximately 81% (n = 89) of total deliveries were by cesarean section. Only 2 mothers (1.8%) smoked during pregnancy, and 7 mothers (6.4%) had smoked before pregnancy. Further, 3.6% of mothers (n = 4) experienced gestational diabetes mellitus, 22.7% (n = 25) had chorioamnionitis, 10% (n = 11) had idiopathic premature rupture of the membrane without inflammation (hereinafter referred to as iPROM), and 18.2% (n = 20) experienced preeclampsia.

Covariates associated with GA and/or birth weight SD scores.

We evaluated the association between pregnancy- and delivery-related variables, infant sex, and GA at birth and/or birth weight SD scores for GA (hereinafter referred to as SD scores). Higher SD scores were associated with older GA (Fig. 1, Supplementary Tables 2, 3; $p < 0.05$). Male infants, cesarean section, higher maternal pre-pregnancy BMI, maternal smoking before pregnancy, and chorioamnionitis were all associated with earlier GA (Fig. 1a; $p < 0.05$). Moreover, there was a suggestive association between iPROM and earlier GA (Fig. 1a; $p = 0.060$), and preeclampsia was associated with lower SD scores (Fig. 1b; $p < 0.05$). In multivariate analysis that considered these variables, the direction of effect remained similar, and the association with iPROM and preeclampsia became stronger (Supplementary Table 4, 5).

Epigenome-wide association study on GA and/or birth weight SD scores using cord blood samples and pathway analysis.

The EWAS of GA and SD scores using the cord blood samples utilized two linear regression models that differed in the extent of covariate adjustment. Using the false discovery rate (FDR) correction[21] for multiple testing (q < 0.05, 410,735 tests), based on "Model 1" we identified 43,930 CpG sites associated with GA and 658 CpGs associated with SD score (Fig. 2a,b; Supplementary Fig. 6a, 7a). Based on "Model 2" that adjusted for additional covariates, we identified 29,071 sites associated with GA and 163 sites associated with SD score (Fig. 2a,b; Supplementary Fig. 6b, 7b). We considered candidate CpGs as those associated with GA or SD scores in both models in the same direction, resulting in the identification of 27,619 GA-related CpGs and 150 SD score-related CpGs (Supplementary Tables 6 and 7). We pursued a sensitivity analysis approach used similarly in previous studies to assess whether associations were captured sufficiently from "Model 2″ which contained six additional prenatal covariates[22]. Regression analysis were pursued adjusting for "Model 1″ covariates in addition to each of these six covariates, in turn, and the number of associated CpGs were observed. Results of all sensitivity analyses (FDR < 0.05) showed overlap of 26,202 GA-related CpGs (95%) and 141 SD score-related CpGs (94%), all of which were included in the larger set of 27,619 GA-related and 150 SD score-related CpGs (Supplementary Table 8, 9). Additionally, we categorized both groups of CpGs based on directionality of the regression coefficients. GA-related CpGs consisted of 17,260 positively related sites and 10,359 negatively related sites (Fig. 2a,c; Supplementary Table 6). SD score-related CpGs consisted of 113 positively related sites and 37 negatively related sites (Fig. 2b,d; Supplementary Table 7). GA-related CpGs

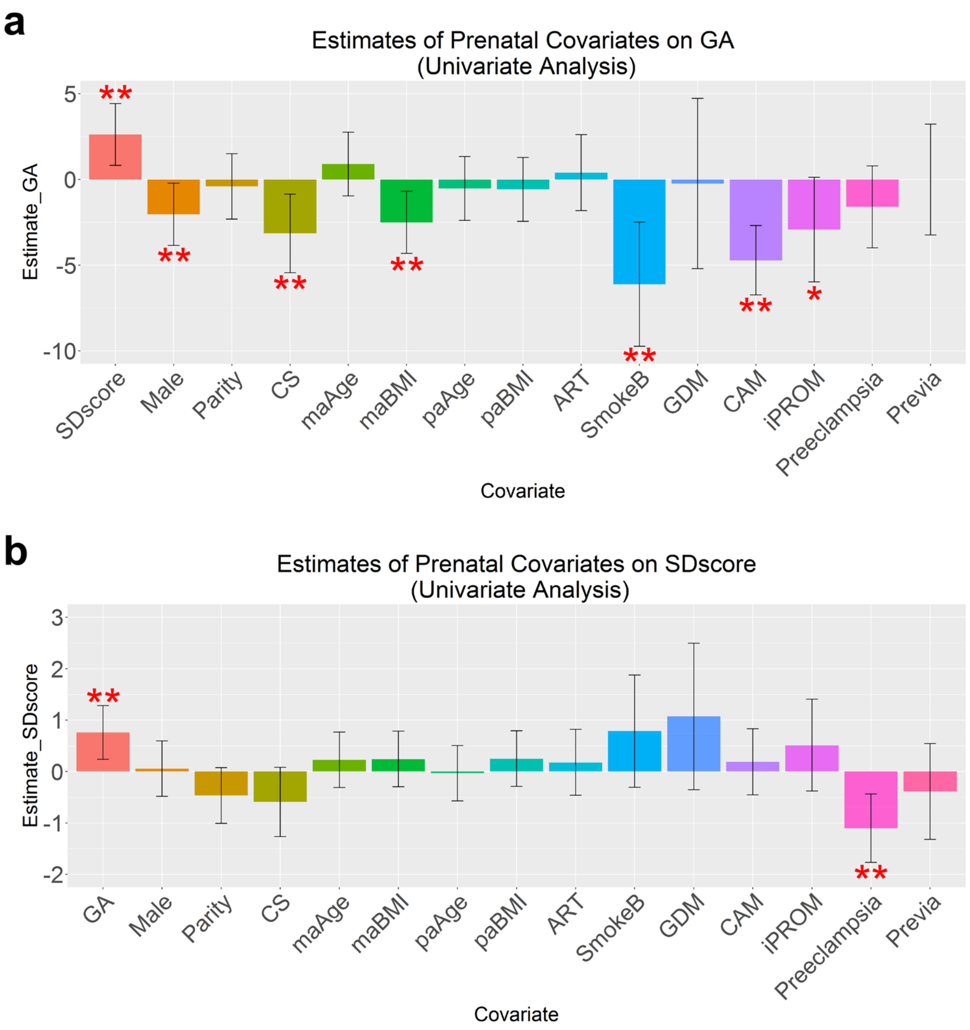

Figure 1. Association of prenatal covariates with gestational age and/or birth weight SD scores (n = 110, cord blood samples). (**a**) Association of prenatal covariates with gestational age (GA). Red asterisks with each covariate represent *p*-values for association between predictor (GA or birth weight SD score) and prenatal covariate (double red asterisks = *p* value < 0.05 (univariate linear regression analysis); single red asterisk = *p* value of 0.060 (suggestive)). Regression coefficients (Estimates) and *p* values are reported as a week's change in GA for two standard deviation increases in continuous prenatal variables, or for comparing the two categories of binary prenatal variables. Error bars indicate 95% confidence interval of effect size. (**b**) Associations of prenatal covariates with birth weight SD scores. Estimates are reported as changes in birth weight SD scores for two standard deviation increases in continuous prenatal variables, or for comparing the two categories of binary prenatal variables. Abbreviations & which covariate is continuous or binary: [Continuous covariates] *GA*: gestational age, *SD score*: birth weight SD score, *maAge*: maternal age, *maBMI*: maternal pre-pregnancy BMI, *paAge*: paternal age, *paBMI*: paternal BMI [Binary covariates] *Male*, *Parity* (> 0 or 0), *CS*: cesarean section, *ART* : assisted reproductive technology, *SmokeB*: maternal smoking before pregnancy, *GDM*: gestational diabetes mellitus, *CAM*: chorioamnionitis, *iPROM*: idiopathic premature rupture of the membrane, *Preeclampsia*, *Previa*: placenta previa.

were more likely to be located in CpG island shores ($p < 2.2e{-}16$), the distribution of which was 1.4-fold more than that of all CpGs contained in the HumanMethylation450 BeadChip (hereinafter referred to as 450 k array) (Supplementary Fig. 8). The distribution of SD-score-related CpGs at open sea ($p = 6.9e{-}08$) was 1.5-fold more than that of all CpGs contained in 450 k array.

For KEGG pathway enrichment analysis, we selected genes in which the promoter region had at least 2 CpGs associated with GA or SD scores. The DAVID bioinformatics resources[23] found no FDR-significant associations with genes containing SD score-related CpGs (Fig. 2d). Regarding GA-related CpGs, 9 pathway categories were significantly enriched in the analysis for positively GA-related CpGs, and 27 pathway categories were significantly enriched in the analysis for negatively GA-related CpGs after filtering for enrichment-FDR ≤ 0.1 (Supplementary Table 10). The terms indicating inflammation (for example, "inflammatory bowel disease"), "cytokine-cytokine receptor interaction", and "NF-kappa B signaling pathway" were enriched in the analysis for negatively GA-related

Prenatal variable	Mean (SD)	Median	N (%)
Sex (Male)			53 (48.2)
Maternal age	33.8 (4.7)	34	
< 25 years			1 (0.9)
25 ~ 30 years			20 (18.2)
30 ~ 35 years			41 (37.3)
35 ~ 40 years			34 (30.9)
> 40 years			14 (12.7)
Maternal pre-pregnancy BMI	21.1 (3.5)	20.3	
< 18.5 kg/m^2			23 (20.9)
18.5 ~ 25 kg/m^2			77 (70.0)
25 ~ 30 kg/m^2			4 (3.6)
> 30 kg/m^2			6 (5.5)
Parity (> 0)			43 (39.1)
Smoking during pregnancy (Yes)			2 (1.8)
Smoking before pregnancy (Yes)			7 (6.4)
Assisted reproductive technology (ART: Yes)			25 (22.7)
Gestational diabetes mellitus (Yes)			4 (3.6)
Preeclampsia (Yes)			20 (18.2)
Placenta previa (Yes)			10 (9.1)
Chorioamnionitis (CAM: Yes)			25 (22.7)
Idiopathic premature rupture of the membrane (iPROM: Yes)			11 (10.0)
Delivery mode (cesarean section)			89 (80.9)
Gestational age at birth	34.0 (4.9)	35	
< 28 weeks			17 (15.5)
28 ~ 32 weeks			17 (15.5)
32 ~ 37 weeks			31 (28.2)
> 37 weeks			45 (40.9)
Birth weight SD score	− 0.6 (1.4)	− 0.5	
< − 2.5			16 (14.5)
− 2.5 to − 1.28			22 (20.0)
− 1.28 to 1.28			60 (54.5)
1.28 ~ 2.5			12 (10.9)

Table 1. Pregnancy- and delivery-related characteristics of 110 mother-infant pairs. *Since the table containing all the values exceeds one page, other descriptive characteristics that cannot be written in Table are shown in Supplementary Table 1.

CpGs, whereas "ECM-receptor interaction" and "PI3K-Akt signaling pathway" were enriched in the analysis for positively GA-related CpGs (Fig. 2e,f).

Association analysis of transcription and GA and/or birth weight SD scores and pathway analysis. Among the 27,701 CpGs associated with GA and/or birth weight SD scores in the cord blood EWAS, we matched 15,038 CpGs to 7,369 QC-filtered gene expression probes within a region of 250 kb upstream or downstream of CpGs (Fig. 3a,b). Association analysis was performed on these 7,369 transcripts which resulted in the identification of 461 FDR-significant GA-related transcripts (1,611 nominally significant transcripts; nominal p-value < 0.05). Among these GA-related transcripts, 220 were negatively related (680 at a nominal $p < 0.05$) and 241 were positively related (931 at a nominal $p < 0.05$) (Fig. 3c; Supplementary Table 11). In contrast, there were no FDR-significant transcripts associated with birth weight SD score, but six were nominally significant transcripts (Fig. 3d; Supplementary Table 12).

When we conducted pathway enrichment analysis for FDR-significant GA-related transcripts, five pathway categories were significant all of which were confined to only the negatively GA-related transcripts (enrichment-FDR ≤ 0.1) (Supplementary Table 13). Enrichment analysis applied to the nominally significant GA-related transcripts resulted in 8 significantly enriched pathway categories among the negatively GA-related expression genes, and 20 significantly enriched pathway categories among the positively GA-related sites (Supplementary Table 14). Some pathway categories were simultaneously ranked within the list of top 10 enriched pathways appropriately in opposite directions in the GA-CpG methylation analysis and GA-expression analysis. The following pathway categories were ranked in both the top 10 lists of negatively GA-related CpGs and positively GA-related transcripts: inflammatory bowel disease, viral myocarditis, NF-kappa B signaling pathway, and allograft rejection. In contrast, the following pathway categories ranked in both top 10 lists of positively GA-related CpGs and negatively GA-related transcripts: ECM-receptor interaction, PI3K-Akt signaling pathway, Rap1 signaling pathway, and focal adhesion (Figs. 2e,f, 3e,f; Supplementary Table 14).

Confirmation of direct association between DNA methylation and gene expression with methylation expression analysis. Based on the results of cord blood EWAS and association analysis of transcription, we generated 1,355 CpG-transcript combinations connected with 461 GA-related expression probes and 1,196 GA-related CpGs within 414 RefSeq genes. From the cord blood samples, 55 were available for investigating direct methylation-expression relationships (Supplementary Fig. 9a). Within the 1,355 CpG-transcript combinations, significant associations between CpG methylation and gene expression were confirmed in 757 combinations (nominal $p < 0.05$) (Supplementary Fig. 9c, Supplementary Table 15). This corresponded to 674 GA-related CpGs showing significant methylation expression correlations to 281 RefSeq genes (Fig. 4a). Among these 674 CpG sites, 409 CpGs (458 combinations) showed negative correlation between % methylation and $\log_2$ expression values, while 265 CpGs (299 combinations) showed a positive correlation (Fig. 4b). Within the 674 CpG sites, 84 in the promoter regions (including TSS200, TSS1500, 5′UTR, 1st Exon) showed positive correlation between % methylation and $\log_2$ expression, thus exhibiting a 'discordant' relation[24] where transcription increased when methylation increased (Fig. 4b, green dots). In comparison, 'concordant' relation was confirmed in 165 promoter CpGs, where transcription decreased when methylation increased. Within the 'discordant' promoter CpGs, "Repressed Polycomb" occupied the highest proportion (22.6%) among the 25 chromatin states of cord blood T cell-based annotation imputed by ChromHMM[25], with an enrichment odds ratio of 3.8 when compared to the reference proportion based on all CpGs contained in 450 k array (Fig. 4c,d; Supplementary Table 16). We listed the genes in which methylation levels were related to GA at multiple CpGs within the same genes from 84 discordant promoter CpGs (Fig. 4e). *UCN* was the top-ranked gene based on the largest number of CpGs included in the 84 discordant promoter CpGs, and whose promoter was occupied by "Repressed Polycomb" in most types of blood cells except for hematopoietic stem cells (Fig. 4f., E035, E051). Promoters in hematopoietic stem cells were occupied by bivalent promoter states which was in common with H1 embryonic stem cells (Fig. 4f., E003). Indeed, both the methylation in the promoter CpG of *UCN* (cg13833437) and the expression of *UCN* were significantly correlated to GA (Fig. 4g,h), in addition to positive correlation between methylation and expression levels (Fig. 4i). Within the 165 'concordant' promoter CpGs, "Promoter upstream TSS" occupied the highest proportion (22.4%) among the 25 chromatin states of cord blood T cell-based annotation imputed by ChromHMM, with an enrichment odds ratio of 2.4 when compared to the reference proportion based on all CpGs contained in the 450 k array (Supplementary Table 17). *CARD11* was the top-ranked gene based on the largest number of CpGs included in the 165 'concordant' promoter CpGs (Supplementary Fig. 10), and *CARD11* promoter was occupied by "Promoter upstream TSS".

Candidate CpGs for GA-involved epigenetic memory. To evaluate whether GA at birth was still associated with DNA methylation in postnatal peripheral blood cells, we conducted EWAS using postnatal blood DNA methylation values. Postnatal blood samples for analysis were collected around their expected due dates from 47 babies whose cord blood samples were utilized for DNA methylation analysis. The GA EWAS was repeated among these 47 cord blood samples, and association with GA at birth was also examined in relation to DNA methylation in their postnatal samples. We identified 8,484 and 0 FDR-significant CpGs associated with GA in cord blood and postnatal peripheral blood, respectively. The volcano plot showing the regression coefficients of the DNA methylation and GA association was V-shaped for the 47 cord blood samples analyzed (Supplementary Fig. 11a), similar to the analysis using 110 samples (Fig. 2c). In contrast, the volcano plot based on the postnatal peripheral blood samples indicated no evidence of an association (Supplementary Fig. 11b).

Next, we examined the relationship between DNA methylation at birth and methylation postnatally around the expected due date. Pearson's correlation coefficients between 47 paired cord and postnatal peripheral blood mononuclear cell methylation values were calculated for all 27,619 GA-related CpGs identified in the first EWAS of 110 cord blood samples. The median time interval between the two blood draws was 7.1 weeks (range: 2.0 to 18.1 weeks). We considered CpGs of correlation coefficient ≥ 0.7 as the candidates for GA-involved epigenetic memory, similar to definitions used in previous reports[19]. We identified 2,093 candidate CpGs for GA-involved epigenetic memory that showed a correlation coefficient ≥ 0.7 (Fig. 5a; Supplementary Table 18). Among these, CpGs showing high methylation at birth were likely to remain high after the birth as well, while those of low methylation values at birth appeared to remain low after birth (Fig. 5b). To evaluate the possibility that the correlation coefficients may be influenced by the time interval of the two blood draws, we ordered the samples by time interval and compared the correlation coefficients of the bottom 23 samples (median time interval: 4.0 weeks) and top bottom 23 samples (median time interval: 11.0 weeks) by using paired *t*-tests. The mean of the bottom group was only 0.036 (95%CI: (0.030, 0.042)) higher than that of the top group (Supplementary Fig. 12), and the distribution of correlation coefficients of the two groups were similar. High correlations were observed across multiple CpGs in genes such as *UCN* and *RGMA*. The methylation of certain CpGs in these genes were also correlated with neighboring CpGs in cord and postnatal blood samples. This may indicate that specific genomic regions were regulated in the same way during the perinatal period (Fig. 5c). To characterize those regions, we referred to ChromHMM 25-chromatin-states of the 2,093 candidate CpGs for GA-involved epigenetic memory. Among these 2,093 CpGs studied, "Repressed Polycomb" and "Bivalent Promoter" showed as the second and the third highest frequency after "Quiescent/Low" in both cord blood T cell-based and B cell-based annotations (Fig. 5d; Supplementary Fig. 13, Supplementary Table 19). These two chromatin states were also enriched in Fisher's exact test in both annotations, and "Repressed Polycomb" was most significantly enriched (Fig. 5e). Further, as the correlation coefficients between cord blood and postnatal blood DNA methylation increased, the proportion of loci occupied by "Repressed Polycomb" or "Bivalent Promoter" increased as

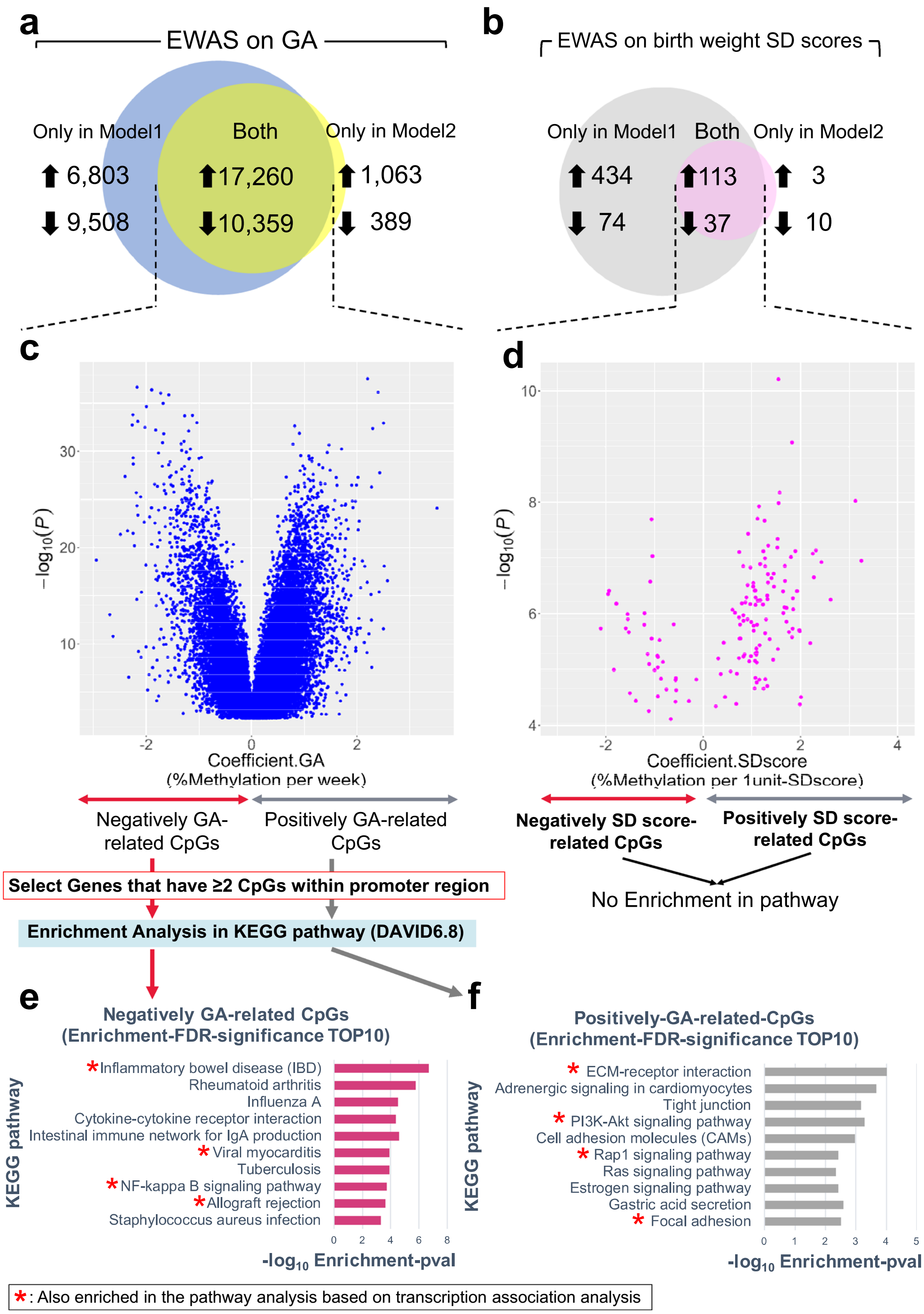
a
EWAS on GA
Only in Model1
Both
Only in Model2
⬆6,803
⬇9,508
⬆17,260
⬇10,359
⬆1,063
⬇389
b
EWAS on birth weight SD scores
Only in Model1
Both
Only in Model2
⬆434
⬇74
⬆113
⬇37
⬆3
⬇10
c
−log10(P)
30
20
10
-2
0
2
Coefficient.GA
(%Methylation per week)
d
−log10(P)
10
8
6
4
-2
0
2
4
Coefficient.SDscore
(%Methylation per 1unit-SDscore)
Negatively GA-related CpGs
Positively GA-related CpGs
Negatively SD score-related CpGs
Positively SD score-related CpGs
No Enrichment in pathway
Select Genes that have ≥2 CpGs within promoter region
Enrichment Analysis in KEGG pathway (DAVID6.8)
e
Negatively GA-related CpGs
(Enrichment-FDR-significance TOP10)
KEGG pathway
*Inflammatory bowel disease (IBD)
Rheumatoid arthritis
Influenza A
Cytokine-cytokine receptor interaction
Intestinal immune network for IgA production
*Viral myocarditis
Tuberculosis
*NF-kappa B signaling pathway
*Allograft rejection
Staphylococcus aureus infection
0
2
4
6
8
-log10 Enrichment-pval
f
Positively-GA-related-CpGs
(Enrichment-FDR-significance TOP10)
KEGG pathway
* ECM-receptor interaction
Adrenergic signaling in cardiomyocytes
Tight junction
* PI3K-Akt signaling pathway
Cell adhesion molecules (CAMs)
* Rap1 signaling pathway
Ras signaling pathway
Estrogen signaling pathway
Gastric acid secretion
* Focal adhesion
0
1
2
3
4
5
-log10 Enrichment-pval
*: Also enriched in the pathway analysis based on transcription association analysis

◂**Figure 2.** Epigenome-wide association study (EWAS) of gestational age and/or birth weight SD scores (n = 110, cord blood samples). (**a**) Blue circle reflects CpGs associated with gestational age (GA) in "Model 1" linear regression analysis and yellow circle reflects CpGs in "Model 2". The intersection of blue and yellow circles means finally decided CpGs associated with GA. Upward (or downward) arrows mean the number of CpGs whose methylation increases (or decreases) when predictor values increase. (**b**) Gray circle reflects CpGs associated with birth weight SD score in Model 1 linear regression analysis and pink circle reflects CpGs in Model 2. The intersection of gray and pink circles means finally decided CpGs associated with birth weight SD score. (**c**) Volcano plot indicating regression coefficients (x-axis) versus *p*-values (-$\log_{10}$ scale) of CpGs associated with GA. All values were generated in Model 1 analysis. (**d**) Volcano plot indicating regression coefficients (x-axis) versus *p* values (-$\log_{10}$ scale) of CpGs associated with birth weight SD scores. All values were generated in Model 1 analysis. (**e**) Top 10 KEGG pathway categories enriched in the gene set of negatively GA-related CpGs by using DAVID 6.8. We selected genes in which the promoter region had at least 2 CpGs associated with GA. Single red asterisk denotes a pathway category which was also enriched in GA-related transcripts. x-axis of the barplots means $-\log_{10}$ enrichment *p*-value. (**f**) Top 10 KEGG pathway categories enriched in the gene set of positively GA-related CpGs by using DAVID 6.8. *Model 1) *objective variable*: %methylation, *predictors*: GA, SD-score, *adjusted for*: infant sex, batch, cell proportion. **Model 2) *objective variable*: %methylation, *predictors*: GA, SD-score, *adjusted for*: infant sex, batch, cell proportion, chorioamnionitis, idiopathic premature rupture of the membrane, preeclampsia, maternal smoking before pregnancy, maternal pre-pregnancy BMI, cesarean section. ***GA: gestational age, *SD-score*: birth weight SD score, *EWAS*: epigenome-wide association study.

well (Fig. 5g). Indeed, CpGs in *UCN* and *RGMA*, where the DNA methylation levels of each CpG correlated well with neighboring CpGs, were mainly in a state of "Repressed Polycomb" and "Bivalent Promoter", respectively (Figs. 4f, 5c). Apart from these two genes, multiple CpGs in *PRDM16*, *SLC38A4*, and *ZSCAN12L1*, which were included in the 2,093 candidate CpGs for GA-involved epigenetic memory, were also in a state of "Repressed Polycomb" and/or "Bivalent Promoter" (Fig. 5f).

Finally, we investigated transcription of the aforementioned candidate CpGs for GA-involved epigenetic memory. Of the 2,093 candidate CpGs, 54 had methylation expression correlation in cord blood (Fig. 5h), where half of the CpGs had a negative correlation and the other half had a positive correlation (Supplementary Table 20). From these 54 CpGs, 8 CpGs located in *UCN* were identical to the ones in the multiple 'discordant' promoter CpGs of Fig. 4e. Thus, cord blood DNA methylation of 8 CpGs in the *UCN* promoter were GA-related, positively correlated with expression, and also correlated with own postnatal blood methylation. However, 97.4% of the 2,093 candidate CpGs showed no methylation expression correlation at birth in cord blood.

Discussion

In this study, 27,619 GA-related CpGs and 150 SD score-related CpGs were initially identified from the cord blood EWAS. Secondly, 461 GA-related transcripts and no SD score-related transcripts were found, and methylation expression correlations among approximately two-thirds of GA-related CpG transcript combinations were observed. Lastly, 2093 candidate CpGs for GA-involved epigenetic memory were identified. Among these candidates, trends of chromatin states, such as, "Repressed Polycomb" was observed, alongside the confirmation of 54 CpG correlations with transcription, and the non-negligible number of discordant CpGs where transcription increased as methylation increased.

Four studies have previously been conducted on GA-related CpGs and/or GA-prediction CpGs. More than 75% of the GA-related CpGs reported by Schroeder et al. (41 CpGs identified in a discovery cohort, 26 of which replicated[13]) or ARIES Cohort (224 CpGs[15]) were also identified in our study. On the other hand, only approximately 40% of our 27,619 GA-related CpGs were found among the 44,359 CpGs associated with ultrasonography-determined GA (Bohlin et al.) within the MoBa Cohort data[17] (Supplementary Fig. 14). However, regarding RefSeq genes within 250 bp upstream or downstream to CpGs, approximately 80% of our GA-related RefSeq genes were common to the Bohlin et al. study. The discrepancy of CpG loci between the present study and Bohlin et al. study may be attributed to racial differences (Japanese vs Norwegian) and/or sampling methods used (mononuclear cell separation (lymphocyte-dominant) vs buffy coat without additional cell isolation (granulocyte-dominant)). Of the 131 CpGs for GA-prediction identified by Bohlin et al.[17], 108 were found among our GA-related CpGs while 50 of 148 CpGs reported by Knight et al.[16] (using the method developed by Horvath[26]) were observed in our study (Supplementary Fig. 15). The difference in overlap between studies may be attributed to the selection methods of GA-prediction CpGs. In contrast, our transcription-correlated GA-related CpGs or epigenetic memory candidate CpGs overlapped only minimally with the aforementioned prediction CpGs. Thus, most epigenetic memory candidate CpGs may not be suitable for predicting accurate GA, which may be reasonable based on the understanding that memory methylation would not undergo changes *ex utero* according to chronological time passing.

The CpGs associated with birth weight in previous studies (Engel et al., MoBa; Simpkin et al., ARIES)[15,18] or CpGs associated with "birth weight SD score for GA"[19] were not observed among birth weight SD score-related CpGs in our study. One reason for such discrepancies may lie with this study's participant population whose ratio of preterm to term infants was approximately 1.5, whereas the previous studies pertained mainly to term infants. Second, the results may be affected by differences in nutritional and environmental status of mothers between the study areas. For instance, Japanese mothers are likely to have less body-weight gain during pregnancy than mothers in other countries[27].

There are several strengths to note compared with previous cord blood EWAS of GA. Firstly, we conducted an integrative analysis of the methylome and simultaneously generated transcription data. Secondly, we evaluated

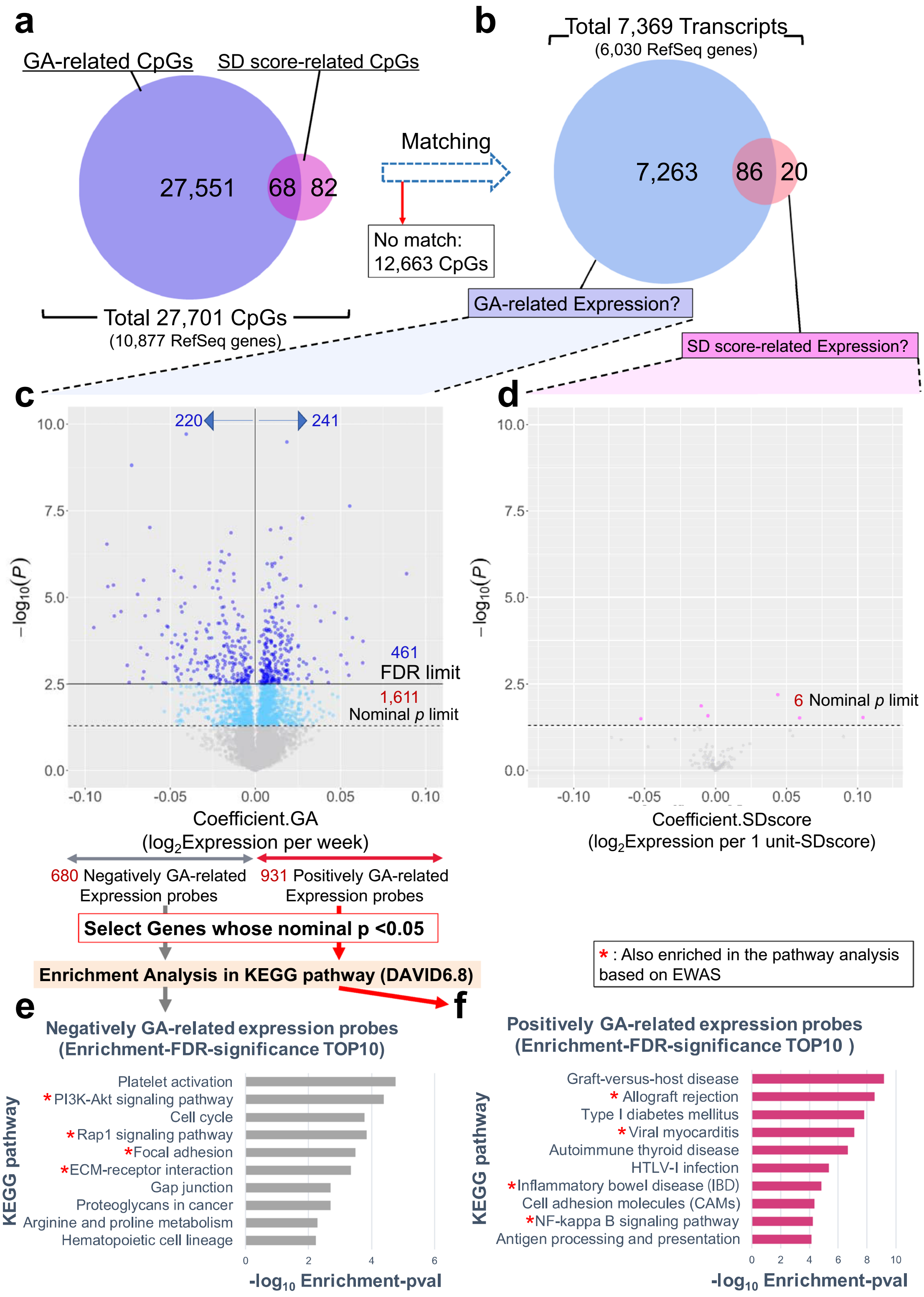
a
GA-related CpGs
SD score-related CpGs
27,551
68
82
Total 27,701 CpGs
(10,877 RefSeq genes)
Matching
No match:
12,663 CpGs
b
Total 7,369 Transcripts
(6,030 RefSeq genes)
7,263
86
20
GA-related Expression?
SD score-related Expression?
c
220
241
10.0
7.5
5.0
2.5
0.0
$-\log_{10}(P)$
461
FDR limit
1,611
Nominal *p* limit
-0.10
-0.05
0.00
0.05
0.10
Coefficient.GA
($\log_2$Expression per week)
d
10.0
7.5
5.0
2.5
0.0
$-\log_{10}(P)$
6 Nominal *p* limit
-0.10
-0.05
0.00
0.05
0.10
Coefficient.SDscore
($\log_2$Expression per 1 unit-SDscore)
680 Negatively GA-related Expression probes
931 Positively GA-related Expression probes
Select Genes whose nominal p <0.05
Enrichment Analysis in KEGG pathway (DAVID6.8)
* : Also enriched in the pathway analysis based on EWAS
e
Negatively GA-related expression probes
(Enrichment-FDR-significance TOP10)
KEGG pathway
Platelet activation
*PI3K-Akt signaling pathway
Cell cycle
*Rap1 signaling pathway
*Focal adhesion
*ECM-receptor interaction
Gap junction
Proteoglycans in cancer
Arginine and proline metabolism
Hematopoietic cell lineage
0
2
4
6
$-\log_{10}$ Enrichment-pval
f
Positively GA-related expression probes
(Enrichment-FDR-significance TOP10)
KEGG pathway
Graft-versus-host disease
* Allograft rejection
Type I diabetes mellitus
*Viral myocarditis
Autoimmune thyroid disease
HTLV-I infection
*Inflammatory bowel disease (IBD)
Cell adhesion molecules (CAMs)
*NF-kappa B signaling pathway
Antigen processing and presentation
0
2
4
6
8
10
$-\log_{10}$ Enrichment-pval

◂**Figure 3.** Association analysis of transcription and gestational age and/or birth weight SD score (n = 55, cord blood samples). (**a**) Blue circle reflects CpGs associated with gestational age in cord blood EWAS and pink circle reflects CpGs associated with birth weight SD scores. (**b**) 19,640 among 27,701 CpGs detected in cord blood EWAS were matched to 9,691 gene expression microarray probes. Light blue circle reflects gene expression probes matched to GA-related CpGs, and pink circle reflects probes matched to SD score-related CpGs. (**c**) Volcano plot indicating regression coefficients (x-axis) versus *p*-values (-$\log_{10}$ scale) of gene expression probes associated with GA. All values were generated in the multivariate linear regression analysis*. Deep blue dots mean FDR-significant. Light blue dots mean nominal $p < 0.05$ and FDR ≥ 0.05. Grey dots mean nominal $p \geq 0.05$. (**d**) Volcano plot indicating regression coefficients (x-axis) versus *p*-values (-$\log_{10}$ scale) of gene expression probes associated with birth weight SD scores. All values were generated in Model1 analysis. Pink dots mean nominal $p < 0.05$ and FDR ≥ 0.05. Grey dots mean nominal $p \geq 0.05$. (**e**) Top 10 KEGG pathway categories enriched in negatively GA-related expression probes by using DAVID 6.8. Here, threshold of selecting expression probes is nominal $p < 0.05$. Single red asterisk denotes a pathway category which was also enriched in GA-related CpGs. x-axis of the barplots means $-\log_{10}$ enrichment *p*-value. (**f**) Top 10 KEGG pathway categories enriched in positively GA-related expression probes by using DAVID 6.8. *Analysis model) *objective variable*: $\log_2$-transformed expression of each gene expression probes, *predictors*: GA, SD score, *adjusted for*: infant sex, batch, cell proportion. *******GA*: gestational age, *SD score*: birth weight SD score, *EWAS*: epigenome-wide association study.

methylation persistence between samples at birth and samples at the expected due date, and among the CpGs of persistent methylation we discovered novel trends in chromatin state and transcription.

Although there have been previous reports on GA-related CpGs, we also identified 461 GA-related transcripts by using the same samples as those used in the EWAS of GA. In addition, the NF-kappa B signaling pathway was enriched in both negatively GA-related CpGs and positively GA-related transcripts while the PI3K-Akt signaling pathway was enriched in the inverted manner. These relationships are consistent with the accepted notion that higher methylation in promoter region leads to repressed gene expression, thereby supporting the validity of our analyses. Correlations between methylation and transcription were confirmed in approximately 2/3 of GA-related transcripts. Among these correlated CpG-transcript combinations, the combinations of positive correlations were found in approximately half as many as negatively correlated combinations – a non-negligible number. In the promoter region, positive correlation between methylation and transcription means a discordant CpG-transcript relation where transcription increases as methylation increases. Recent studies targeting other sample types revealed that CpGs of such discordant relation are not uncommon[24,28]. In the present study, "Repressed Polycomb" of the 25 chromatin states in ChromHMM had the highest number among discordant promoter CpGs. It was also reported that the relation between methylation and transcription at the polycomb-binding site could be opposite from that of other sites[29,30].

With respect to GA-involved epigenetic memory, we identified 2,093 candidate CpGs based on a correlation coefficient ≥ 0.7 between cord and postnatal blood methylation, although we did not identify any FDR-significant CpGs in the postnatal blood EWAS whose methylation was associated with GA at birth. These results suggest that some epigenetic effects of preterm birth may tend to persist postnatally, but there may be fluctuations in the degree of epigenetic memory. Also, methodologically, the lack of significant CpGs may have been due to limited statistical power. Furthermore, we demonstrated that the states of "Repressed Polycomb" and "Bivalent Promoter" were enriched among the GA-related epigenetic candidate CpGs. These two types of chromatin states are based on the repressive histone mark of H3K27me3[25], or related to polycomb-binding, and are closely connected[31]. Polycomb-binding, or histone modification of H3K27me3, is involved in epigenetic memory in plants[32,33]. GA-involved epigenetic memory candidate CpGs did not necessarily show relationship between methylation and corresponding transcription, with only 54 candidate CpGs found to have significant correlation with gene expression. There were also 11 discordant promoter CpGs among these 54 sites (Supplementary Table 20). *UCN*, *SLC12A7*, *TNFAIP2*, *ANGPT2*, and *NGF* were the only genes within 250 bp upstream or downstream of regions that contained ≥ 3 CpGs and showed an association with GA, correlation with transcription, and correlation coefficient ≥ 0.7 between birth and at around due date. *UCN* showed the largest number of significant CpGs. The EWAS by Bohlin et al. identified multiple GA-related CpGs of *UCN*, *SLC12A7*, and *NGF* by using MoBa cohort data[17], and among them cg20442078 and cg05231308 of *UCN* were also found in our list of transcription-correlated GA-involved epigenetic memory candidates (Supplementary Table 20). *UCN* encodes Urocortin, an endogenous peptide hormone belonging to the corticotropin-releasing hormone (CRH) family[34]. Urocortin is found in the central nervous system (CNS) and peripheral tissues such as the heart, adrenal glands, and lymphocytes. Urocortin influences stress responses in the CNS, cardiovascular system and immune system via CRH receptors 1 or 2. For instance, it has protective effects against myocardial ischemic reperfusion injury[35]. All the loci of *UCN* presented 'discordant' methylation-expression correlations with all these CpGs annotated as "Repressed Polycomb" among the 25 chromatin states. This finding may be possible as discordance has been observed for polycomb-binding sites as described previously. *UCN* was one of the top two genes that had multiple candidate CpGs for GA-involved epigenetic memory with the modification of H3K27me3; the other top gene was *RGMA* whose major chromatin state was 'Bivalent Promoter'. *RGMA* encodes repulsive guidance molecule A, a potent inhibitor of nerve growth that is expressed in several brain diseases, including Alzheimer's disease and multiple sclerosis[36]. *RGMA* has also been reported to play an inhibitory role in cancer progression[37]. Further, a recent study has suggested that *RGMA* may have an important role in the communication between the sympathetic nervous system and inflammation via monocyte activation through the suppression of NF-κB activity and activation of PI3K-Akt-signaling[38].

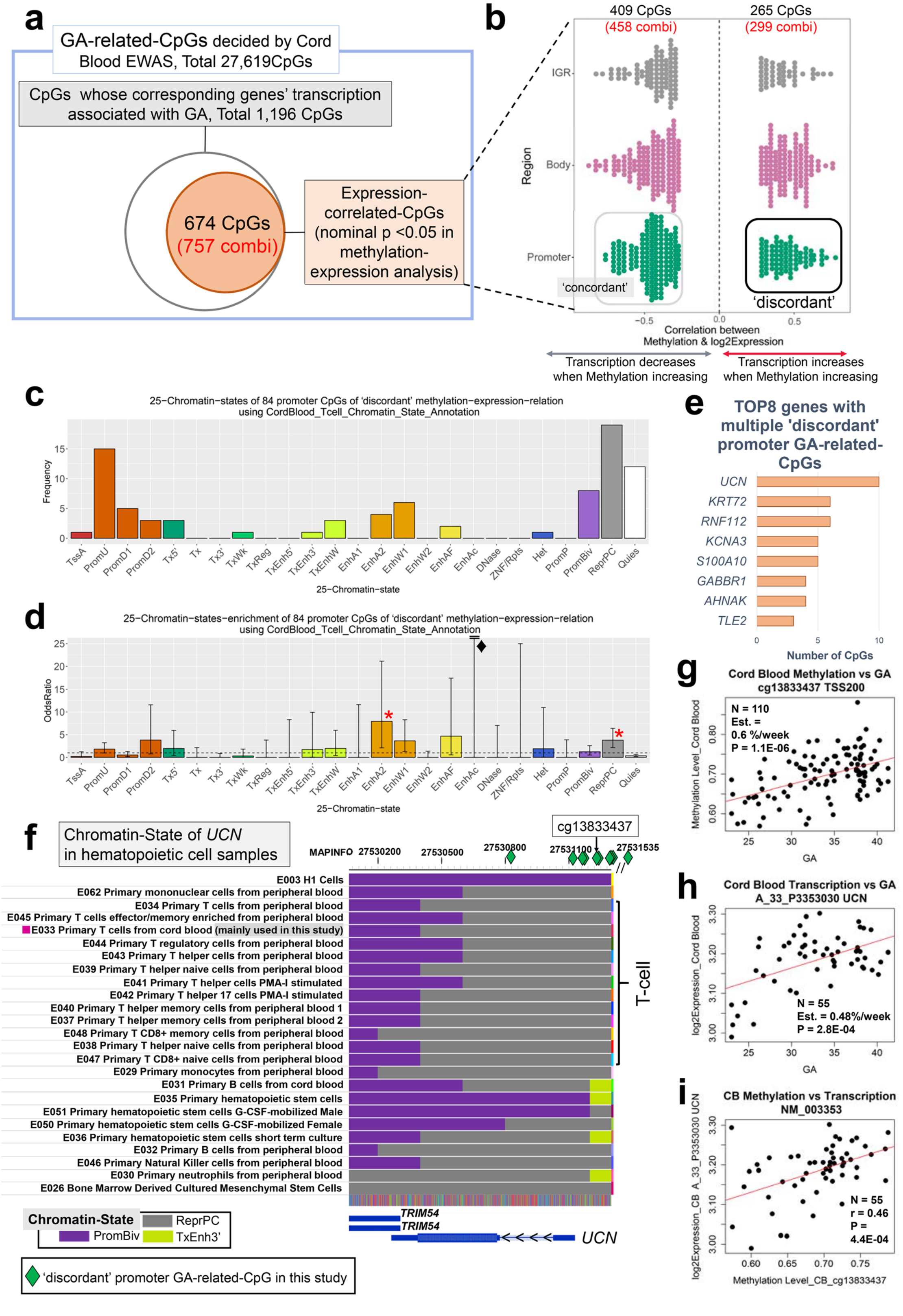
a
GA-related-CpGs decided by Cord Blood EWAS, Total 27,619CpGs
CpGs whose corresponding genes' transcription associated with GA, Total 1,196 CpGs
674 CpGs
(757 combi)
Expression-correlated-CpGs (nominal p <0.05 in methylation-expression analysis)
b
409 CpGs
(458 combi)
265 CpGs
(299 combi)
Region
IGR
Body
Promoter
'concordant'
'discordant'
−0.5
0.0
0.5
Correlation between Methylation & log2Expression
Transcription decreases when Methylation increasing
Transcription increases when Methylation increasing
c
25−Chromatin−states of 84 promoter CpGs of 'discordant' methylation−expression−relation using CordBlood_Tcell_Chromatin_State_Annotation
Frequency
0
5
10
15
TssA
PromU
PromD1
PromD2
Tx5'
Tx
Tx3'
TxWk
TxReg
TxEnh5'
TxEnh3'
TxEnhW
EnhA1
EnhA2
EnhW1
EnhW2
EnhAF
EnhAc
DNase
ZNF/Rpts
Het
PromP
PromBiv
ReprPC
Quies
25−Chromatin−state
d
25−Chromatin−states−enrichment of 84 promoter CpGs of 'discordant' methylation−expression−relation using CordBlood_Tcell_Chromatin_State_Annotation
OddsRatio
0
5
10
15
20
25
*
*
TssA
PromU
PromD1
PromD2
Tx5'
Tx
Tx3'
TxWk
TxReg
TxEnh5'
TxEnh3'
TxEnhW
EnhA1
EnhA2
EnhW1
EnhW2
EnhAF
EnhAc
DNase
ZNF/Rpts
Het
PromP
PromBiv
ReprPC
Quies
25−Chromatin−state
e
TOP8 genes with multiple 'discordant' promoter GA-related-CpGs
UCN
KRT72
RNF112
KCNA3
S100A10
GABBR1
AHNAK
TLE2
0
5
10
Number of CpGs
f
Chromatin-State of UCN in hematopoietic cell samples
cg13833437
MAPINFO
27530200
27530500
27530800
27531100
27531535
E003 H1 Cells
E062 Primary mononuclear cells from peripheral blood
E034 Primary T cells from peripheral blood
E045 Primary T cells effector/memory enriched from peripheral blood
E033 Primary T cells from cord blood (mainly used in this study)
E044 Primary T regulatory cells from peripheral blood
E043 Primary T helper cells from peripheral blood
E039 Primary T helper naive cells from peripheral blood
E041 Primary T helper cells PMA-I stimulated
E042 Primary T helper 17 cells PMA-I stimulated
E040 Primary T helper memory cells from peripheral blood 1
E037 Primary T helper memory cells from peripheral blood 2
E048 Primary T CD8+ memory cells from peripheral blood
E038 Primary T helper naive cells from peripheral blood
E047 Primary T CD8+ naive cells from peripheral blood
E029 Primary monocytes from peripheral blood
E031 Primary B cells from cord blood
E035 Primary hematopoietic stem cells
E051 Primary hematopoietic stem cells G-CSF-mobilized Male
E050 Primary hematopoietic stem cells G-CSF-mobilized Female
E036 Primary hematopoietic stem cells short term culture
E032 Primary B cells from peripheral blood
E046 Primary Natural Killer cells from peripheral blood
E030 Primary neutrophils from peripheral blood
E026 Bone Marrow Derived Cultured Mesenchymal Stem Cells
T-cell
TRIM54
TRIM54
UCN
Chromatin-State
ReprPC
PromBiv
TxEnh3'
'discordant' promoter GA-related-CpG in this study
g
Cord Blood Methylation vs GA
cg13833437 TSS200
N = 110
Est. = 0.6 %/week
P = 1.1E-06
Methylation Level_Cord Blood
0.60
0.70
0.80
25
30
35
40
GA
h
Cord Blood Transcription vs GA
A_33_P3353030 UCN
N = 55
Est. = 0.48%/week
P = 2.8E-04
log2Expression_Cord Blood
3.00
3.10
3.20
3.30
25
30
35
40
GA
i
CB Methylation vs Transcription
NM_003353
N = 55
r = 0.46
P = 4.4E-04
log2Expression_CB A_33_P3353030 UCN
3.00
3.10
3.20
3.30
0.60
0.65
0.70
0.75
Methylation Level_CB_cg13833437

◂**Figure 4.** CpG sites whose methylation correlated with corresponding transcription among gestational age-related CpGs. (**a**) Larger circle with gray line reflects 1,196 CpGs whose corresponding genes' transcription associated with gestational age. Smaller orange circle means 674 CpG sites whose methylation correlated with corresponding transcription $\log_2$-transformed among the 1,196 CpGs (nominal p-value < 0.05; n = 55). 'Combi' means the combinations of the same CpGs and those corresponding transcripts. (**b**) Dot plot indicating the distribution of correlation coefficients between methylation and $\log_2$-transformed gene expression in each of the 3 large regions for the 674 expression-correlated GA-related CpGs. Green dots mean CpGs within "Promoter Region" including TSS1500, TSS200, 5′UTR, 1st Exon. Pink dots mean CpGs within "Gene Body" region including Body, 3′UTR. Black dots mean IGR, *i.e.*, the intergenic region. Regarding "Promoter Region", we defined negative correlation as 'concordant', while positive correlation as 'discordant'. (**c**) Distribution of 25 chromatin states for 84 promoter GA-related CpGs of 'discordant' methylation expression-relation using cord blood T cell-based annotation of ChromHMM. (**d**) Enrichment of 25 chromatin states for 84 promoter GA-related CpGs of 'discordant' methylation expression relation. Error bars indicate 95% CI (confidence interval). Single red asterisk denotes the enriched chromatin state which was significant at Bonferroni-criteria (0.05/25) and of odds ratio ≥ 1 (black dashed line). Filled black diamnod indicate that the upper limit of 95% CI is too high to show in error bars because this value is a prominent outlier, more than 3 times of the 2nd highest value and there is no statistical significance. (**e**). Top 8 genes that have multiple GA-related CpGs of 'discordant' methylation expression relation. **f.** Chromatin state of *UCN* in hematopoietic cell samples. Filled green diamnod means a 'discordant' promoter GA-related CpG, and the representative is cg13833437. (**g**). A scatterplot of GA (x-axis) versus cord blood methylation at cg13833437. (n = 110) (**h**) A scatterplot of GA (x-axis) versus $\log_2$-transformed gene expression of A_33_P3353030, *UCN* transcript (n = 55). (**i**) A scatterplot of methylation of cg13833437 (x-axis) versus $\log_2$-transformed gene expression of A_33_P3353030 (n = 55). **GA*: gestational age. **Chromatin state abbreviations are defined in ChromHMM. Following Abbreviations are defined in ChromHMM; TssA: Active TSS, PromU: Promoter upstream TSS, PromD1: Promoter downstream with DNase, PromD2: Promoter downstream TSS, Tx5′: Transcription 5′, Tx: Transcription, Tx3′: Transcription 3′, TxWk: Weak Transcription, TxReg: Transcription Regulatory, TxEnh5′: Transcription 5′ Enhancer, TxEnh3′: Transcription 3′ Enhancer, TxEnhW: Transcription Weak Enhancer, EnhA1: Active Enhancer 1, EnhA2: Active Enhancer 2, EnhAF: Active Enhancer Flank, EnhW1: Weak Enhancer 1, EnhW2: Weak Enhancer 2, EnhAc: Enhancer Acetylation Only, DNase: DNase only, ZNF/Rpts: ZNF genes & repeats, Het: Heterochromatin, PromP: Poised Promoter, PromBiv: Bivalent Promoter, ReprPC: Repressed Polycomb, Qies: Quiescent/Low.

It is important to acknowledge certain limitations of this study. The sample size was relatively small and varied across the different analyses, and we were not able to attempt replication in an independent cohort. This was largely due to the trade-off between sample size and experimental effort including mononuclear cell isolation and simultaneous DNA/RNA extraction. Despite the modest sample size, we confirmed the same GA-related CpGs found in previous EWAS, identified novel candidates, and were also able to integrate the EWAS findings with transcription data. In the future, it is desirable to evaluate DNA methylation and gene expression simultaneously by using samples from larger populations with plans for replication attempts. Second, the samples for evaluation of epigenetic memory were obtained twice within a short interval between birth and expected due date. A previous study reported that most methylation alteration associated with GA disappears by the age of 7 years[15]. On the other hand, this study successfully demonstrated for the first time that most of these associations were attenuated by around the due date while some epigenetic effects in preterm infants tend to persist at least for several weeks to months. Thus, we consider the use of our postnatally collected samples to be informative in the assessment of epigenetic memory focused on the early life period.

In conclusion, integrative analysis of cord blood methylome and transcription data identified many GA-related methylation alterations and some related to birth weight SD score. We subsequently confirmed methylation expression correlations among candidate CpGs whose methylation was associated with GA. We also identified methylation alterations generated in preterm birth that persisted after birth, thus suggesting GA-involved epigenetic memory. Among these candidate CpGs for epigenetic memory, we found trends of chromatin state such as repressed polycomb-binding sites.

Methods

Ethics statement.

All methods were carried out in accordance with following ethical guidelines in Japan: Ethics Guidelines for Human Genome/Gene Analysis Research, Ethical Guidelines for Medical and Health Research Involving Human Subjects, Ethical Guidelines for Epidemiological Research. Our study was approved by the following institutional ethics committees: Human Genome Ethics Committee of The University of Tokyo Hospital (approval ID: G10036); Ethics Committee of National Center for Child Health and Development (approval ID: 234); Ethics and Personal Information Protection Committee of Tokyo Metropolitan Bokutoh Hospital (approval ID: 38). All participant mothers provided written informed consents for themselves and their infants.

Study population.

We implemented a cross-sectional study design with prospective recruitment of mother-infant pairs considered eligible if they were East Asian, had a live birth at 22–42 weeks gestation, and no fetal congenital disease prenatally diagnosed. Recruitment was targeted for more than 100 mother-infant pairs (median sample size was 96 based on four major previous studies[13,14,20,39]). Between October 2014 and July 2016, 147 mother-infant pairs were invited to participate around the time of delivery at the University of Tokyo Hospital or at the Tokyo Metropolitan Bokutoh Hospital, among which 144 mothers provided written informed

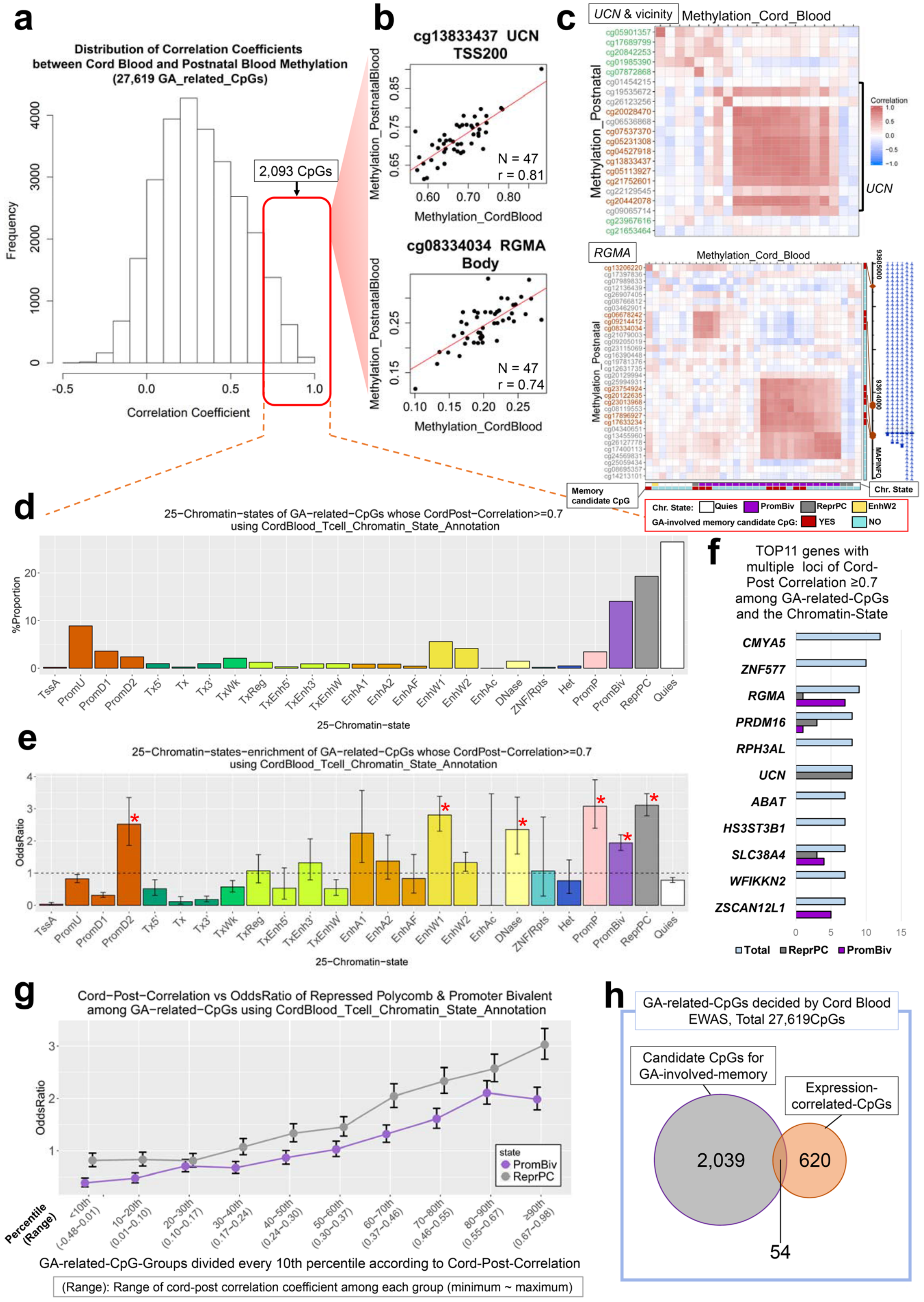
a
Distribution of Correlation Coefficients between Cord Blood and Postnatal Blood Methylation (27,619 GA_related_CpGs)
Frequency
0
1000
2000
3000
4000
-0.5
0.0
0.5
1.0
Correlation Coefficient
2,093 CpGs
b
cg13833437 UCN TSS200
Methylation_PostnatalBlood
0.65
0.75
0.85
0.60
0.70
0.80
Methylation_CordBlood
N = 47
r = 0.81
cg08334034 RGMA Body
0.15
0.25
0.10
0.15
0.20
0.25
N = 47
r = 0.74
c
UCN & vicinity
Methylation_Cord_Blood
Methylation_Postnatal
cg05901357
cg17689799
cg20842253
cg01985390
cg07872868
cg01454215
cg19535672
cg26123256
cg20028470
cg06536868
cg07537370
cg05231308
cg04527918
cg13833437
cg05113927
cg21752601
cg22129545
cg20442078
cg09065714
cg23967616
cg21653464
Correlation
1.0
0.5
0.0
−0.5
−1.0
UCN
RGMA
cg13206220
cg17397836
cg07989833
cg12136439
cg26907405
cg08766812
cg03462901
cg06678242
cg09214412
cg08334034
cg21079003
cg09205019
cg23115069
cg16390448
cg19781376
cg12631735
cg20129994
cg25994931
cg23754924
cg20122635
cg23013968
cg08119553
cg17896927
cg17633234
cg04340651
cg13455960
cg26127778
cg17400113
cg24569831
cg25059434
cg08695357
cg14213101
93605000
93614000
MAPINFO
Memory candidate CpG
Chr. State
Chr. State: □ Quies ▨ PromBiv ▨ ReprPC ▨ EnhW2
GA-involved memory candidate CpG: 🟥 YES ▨ NO
d
25−Chromatin−states of GA−related−CpGs whose CordPost−Correlation>=0.7
using CordBlood_Tcell_Chromatin_State_Annotation
%Proportion
0
10
20
TssA
PromU
PromD1
PromD2
Tx5'
Tx
Tx3'
TxWk
TxReg
TxEnh5'
TxEnh3'
TxEnhW
EnhA1
EnhA2
EnhAF
EnhW1
EnhW2
EnhAc
DNase
ZNF/Rpts
Het
PromP
PromBiv
ReprPC
Quies
25−Chromatin−state
e
25−Chromatin−states−enrichment of GA−related−CpGs whose CordPost−Correlation>=0.7
using CordBlood_Tcell_Chromatin_State_Annotation
OddsRatio
0
1
2
3
4
*
f
TOP11 genes with multiple loci of Cord-Post Correlation ≥0.7 among GA-related-CpGs and the Chromatin-State
CMYA5
ZNF577
RGMA
PRDM16
RPH3AL
UCN
ABAT
HS3ST3B1
SLC38A4
WFIKKN2
ZSCAN12L1
0
5
10
15
□ Total ▨ ReprPC ▨ PromBiv
g
Cord−Post−Correlation vs OddsRatio of Repressed Polycomb & Promoter Bivalent
among GA−related−CpGs using CordBlood_Tcell_Chromatin_State_Annotation
OddsRatio
1
2
3
state
● PromBiv
● ReprPC
Percentile (Range)
<10th (-0.48~0.01)
10~20th (0.01~0.10)
20~30th (0.10~0.17)
30~40th (0.17~0.24)
40~50th (0.24~0.30)
50~60th (0.30~0.37)
60~70th (0.37~0.46)
70~80th (0.46~0.55)
80~90th (0.55~0.67)
≥90th (0.67~0.98)
GA-related-CpG-Groups divided every 10th percentile according to Cord-Post-Correlation
(Range): Range of cord-post correlation coefficient among each group (minimum ~ maximum)
h
GA-related-CpGs decided by Cord Blood EWAS, Total 27,619CpGs
Candidate CpGs for GA-involved-memory
Expression-correlated-CpGs
2,039
620
54

◂**Figure 5.** Candidate CpGs for GA-involved epigenetic memory whose methylation alteration persist after birth. (**a**) Histogram showing distribution of correlation coefficients between cord blood and postnatal blood methylation levels among the 27,619 GA-related CpGs decided by the cord blood EWAS (n = 110). Red block denotes the 2,093 CpGs of correlation coefficients ≥ 0.7 (n = 47), *i.e.*, candidate CpGs whose methylation alteration persist after birth. (**b**) Scatterplots indicating cord blood methylation level (x-axis) versus postnatal blood methylation level for 2 candidate CpGs. These CpGs existed in the representative genes with multiple candidate CpGs in chromatin state of 'Repressed Polycomb' or 'Bivalent Promoter'. (**c**) Heatmap showing Pearson correlation between cord blood and postnatal blood CpG methylation levels in 2 regions (*UCN* with its neighborhood (top panel), the midst of *RGMA* (bottom panel)). Each column (row) represents a cord (postnatal) blood CpG methylation level. Row labels indicate CpG names, and a dark red label means a candidate CpG for epigenetic memory, and a green label means a CpG nearby *UCN*. (**d**) Distribution of 25 chromatin states for GA-related CpGs whose cord-post correlation ≥ 0.7 using cord blood T cell-based annotation of ChromHMM. (**e**) Enrichment of 25 chromatin states for GA-related CpGs whose cord post-correlation ≥ 0.7. Single red asterisk denotes the enriched chromatin state which was significant at Bonferroni-criteria (0.05/25) and of enrichment odds ratio ≥ 1 (black dashed line). (**f**) Top 11 genes with multiple loci of cord-post correlation ≥ 0.7 among GA-related CpGs and those CpGs' chromatin state. (**g**) A line graph showing the relationship between the cord-post correlation level of methylation (x-axis) and the enrichment odds ratio of 2 chromatin states ('Repressed Polycomb', 'Bivalent Promoter'). 27,619 GA-related CpGs were divided into 10 bins every 10th percentile for cord-post correlation coefficients. (**h**) Overlap between 2093 candidate CpGs for GA-involved epigenetic memory (gray circle) and 674 CpGs whose methylation correlated with $\log_2$-transformed expression of corresponding genes (orange circle: see Fig. 4) among GA-related CpGs. **GA*: gestational age, *EWAS*: epigenome-wide association study. **All error bars indicate 95% CI (confidence interval). ***Chromatin state abbreviations are defined in ChromHMM. Following Abbreviations are defined in ChromHMM; TssA: Active TSS, PromU: Promoter upstream TSS, PromD1: Promoter downstream with DNase, PromD2: Promoter downstream TSS, Tx5′: Transcription 5′, Tx: Transcription, Tx3′: Transcription 3′, TxWk: Weak Transcription, TxReg: Transcription Regulatory, TxEnh5′: Transcription 5′ Enhancer, TxEnh3′: Transcription 3′ Enhancer, TxEnhW: Transcription Weak Enhancer, EnhA1: Active Enhancer 1, EnhA2: Active Enhancer 2, EnhAF: Active Enhancer Flank, EnhW1: Weak Enhancer 1, EnhW2: Weak Enhancer 2, EnhAc: Enhancer Acetylation Only, DNase: DNase only, ZNF/Rpts: ZNF genes & repeats, Het: Heterochromatin, PromP: Poised Promoter, PromBiv: Bivalent Promoter, ReprPC: Repressed Polycomb, Qies: Quiescent/Low.

consents, and 3 refused participation (Supplementary Fig. 1). Umbilical cord blood samples were obtained from all participants at the time of infant delivery, and postnatal peripheral blood samples were obtained by venipuncture at least 2 weeks after birth around their due date (36–44 weeks of postmenstrual age). Postnatal blood samples were unavailable for 74 participants for various reasons, but primarily due to hospital discharge occurring prior to 2 weeks after birth (Supplementary Fig. 1).

Covariates. Clinical data (*e.g.* GA, birth weight, mode of delivery, etc.), maternal age and pre-pregnancy BMI, use of assisted reproductive technology (*e.g.* in vitro fertilization (IVF), etc.), mother's smoking status and pregnancy complications, as well as postmenstrual age during postnatal blood collection were obtained from hospital medical records. Paternal data (*i.e.* body weight, height, age) were obtained by questionnaire. Birth weight SD score – namely birth weight z-score for GA according to Japanese reference data – was calculated from GA, birth weight, infants' sex, and parity, through a program provided by the Japanese Society for Pediatric Endocrinology (downloaded from following site on 16th, December, 2016; http://jspe.umin.jp/medical/keisan.html).

Mononuclear cell separation and DNA/RNA extraction. From the obtained blood samples, cord blood mononuclear cells (CBMCs) and peripheral blood mononuclear cell (PBMC) samples were separated by gradient centrifugation using Ficoll-Hypaque within 24 h of sample collection (details are described in Supplementary Fig. 3). The buffy coats of CBMCs/PBMCs were directly lysed with Buffer RLT Plus (Qiagen) containing β-mercaptoethanol in 59 cord blood samples and 14 postnatal blood samples. Genomic DNA was extracted from the lysate of mononuclear cell buffy coat using Qiagen AllPrep kit (Qiagen) (Protocol 1). In the remaining 76 cord blood samples and 52 postnatal blood samples, we utilized Protocol 2, in which the CBMCs/PBMCs buffy coats were processed with erythrocyte lysis solution, and genomic DNA and total RNA were simultaneously extracted from the lysate of the isolated cells using the same kit in Protocol 1. Aliquots of genomic DNA and total RNA were then stored at − 80 °C.

Quality control (QC) and preprocessing in DNA methylation microarray analysis. Following extraction, genomic DNA was bisulfite-converted using the EpiTect Plus DNA Bisulfite Kit (Qiagen). Bisulfited DNA was processed with 450 k array, which can assay methylation levels at more than 485,000 CpG sites. The methylation levels at each CpG site was calculated as β values. The methylation levels at each CpG site was calculated as β values where β = intensity of the methylated allele (*M*) / (intensity of the unmethylated allele (*U*) + intensity of the methylated allele (*M*) + 100). Therefore, β values ranged from 0 (completely unmethylated) to 1 (completely methylated). All methylation data preprocessing was conducted in R environment (v. 3.3.2). The quality of each sample was evaluated using RnBeads package (v. 1.4.0)[40] and *minfi* package (v. 1.20.2)[41]. Failed samples were excluded on the basis of bisulfite conversion efficiency, hybridization efficiency, and the intensity of methylated and unmethylated probes.

After exclusion of low-quality samples, CpG probes were filtered using the ChAMP package (v. 2.6.0)[42]. Non-CpG probes were removed. The probes on the X and Y chromosomes, with a detection p value > 0.01, and a beadcount less than 3 were removed. Based on the default of the ChAMP package, the probes mapping to multiple sites, defined by Nordlund et al.[43], were removed. In addition, according to the data of Chen et al.[44], cross-reactive and polymorphic CpG probes of Asian minor-allele frequency (MAF) ≥ 1% were also removed. After filtering, 410,735 CpG probes remained for further analysis. Background correction and dye-bias equalization (Noob)[45] was then performed using the *minfi* package. To further reduce the bias of type 2 probe values, beta-mixture quantile normalization (BMIQ)[46] was performed using the ChAMP package.

Estimation of cell fraction.

Cell fraction was estimated with the method proposed by Houseman[47,48] using the Bakulski reference data set for cord blood analysis[49]. Estimated cell fraction data including lymphocytes (CD4 + T cells, CD8 + T cells, NK cells, B cells), myelocytes (granulocytes, monocytes), and nucleated red blood cells (nRBCs) were used for further multivariate methylation analysis.

Gene expression microarray analysis and data preprocessing.

Following extraction, total RNA was initially quantified and qualitatively assessed whereby samples with low RNA yield and quality were excluded (Supplementary Fig. 4). Thereafter, 100 ng of total RNA was used to produce Cyanine 3-labeled cRNA. After labeling, 600 ng of cRNA was fragmented and hybridized to the SurePrint G3 Human GE microarray 8 × 60 K Ver. 3.0 (Agilent Technologies). After hybridization, washing the array slides, and scanning, the raw intensity data were obtained using Agilent Feature Extraction (FE) software (ver. 10.7.3.1).

As described in Supplementary Fig. 4, array QC on each sample, probe filtering, and normalization were performed using GeneSpring14.5 (Agilent Technologies). The data set comprised of 65 cord blood and 48 postnatal peripheral blood samples that passed QC; these were then quantile normalized with the minimum expression level of all transcription among all samples set to 1. Probes above the threshold expression criteria were selected, and those on sex chromosomes were removed. Finally, 46,789 probes remained for further analysis. After this preprocessing, the samples from twin infants were excluded. As the number of postnatal blood RNA samples were small, these were not used for further analysis. In total, 55 cord blood RNA samples remained. Prior to transcription analysis, expression probes were selected from among the 46,789 remaining probes according to the results of the cord blood EWAS; probes without threshold background signal detection were removed. The normalized and filtered data were imported into the R environment for statistical analysis.

Statistical analysis.

All statistical analysis was conducted in the R environment (v. 3.3.2). The overall analysis framework is summarized in Supplementary Fig. 5, and the detail of each analysis is described below.

Covariates associating with GA and/or birth weight SD scores.

Simple linear regression analysis was performed to examine the association between prenatal variables and infant GA and birth weight SD scores. Infant sex and six prenatal variables associated with GA and/or birth weight SD scores were included in subsequent analyses. These variables were subject to mutual statistical adjustment in multivariate linear regression analysis of GA and SD scores. As described by Gelman[50] and Lin et al.[51], binary prenatal variables were not scaled, and continuous prenatal variables were standardized to have a standard deviation of 0.5 in order to compare effect estimates from both continuous and binary prenatal variables.

Epigenome-wide association analysis of GA and/or birth weight SD scores and pathway analysis.

Two multivariate linear regression models were used to evaluate the association between GA and SD scores and cord blood DNA methylation value for each CpG site.

$$Y_{meth} = \beta_0 + \beta_{GA} \times X_{GA} + \beta_{SDscore} \times X_{SDscore} + \sum (\beta_i \times X_{COV}) + \varepsilon$$

The two linear regression models differed in covariate adjustment, in which the first model (Model 1) adjusted for infant sex, batch and estimated cellular populations, and the other model (Model 2) additionally adjusted for the above mentioned 6 prenatal covariates associated with GA and/or SD score. To adjust for multiple testing across 410,735 probes, suggestive CpG sites associated with GA or birth weight SD scores were selected at an FDR of < 0.05 in each model. Finally, we defined GA-related CpGs or SD score-related CpGs as CpG sites whose methylation levels were associated with GA or SD scores in both “Model 1” and “Model 2” in the same direction.

In preparations for pathway analyses, we categorized the suggestive CpGs based on the direction of regression coefficients (*i.e.* positive or negative) for both the analysis of GA and SD score, giving rise to four categories of CpGs. Next, the four categories of CpGs were linked to genes using the ChAMP package[23]. In addition to duplicate gene entities, probes lacking an Illumina gene annotation, and probes mapped to gene body, 3′UTR, or intergenic region were not used for pathway analyses. Among the gene entities of each CpG category, only entities with at least 2 CpGs on them were selected. Finally, DAVID Bioinformatics Resources 6.8[23] was used to assess enrichment in KEGG pathway, and Benjamini–Hochberg procedure was applied to this analysis based on the FDR; an enrichment-FDR threshold of ≤ 0.1 was used based on the default applied by the DAVID resource (https://david.ncifcrf.gov/content.jsp?file=functional_annotation.html).

Data availability

Both the methylation microarray data and the gene expression microarray data have been deposited in the Gene Expression Omnibus (GEO) database under accession number GSE110829.

Received: 20 September 2020; Accepted: 28 January 2021
Published online: 09 February 2021

References

1. Barker, D. J. & Osmond, C. Infant mortality, childhood nutrition, and ischaemic heart disease in England and Wales. *Lancet (London, England)* **1**, 1077–1081. https://doi.org/10.1016/S0140-6736(86)91340-1 (1986).
2. Barker, D. J. In utero programming of chronic disease. *Clin. Sci. (London, England: 1979)* **95**, 115–128 (1998).
3. Aarnoudse-Moens, C. S., Weisglas-Kuperus, N., van Goudoever, J. B. & Oosterlaan, J. Meta-analysis of neurobehavioral outcomes in very preterm and/or very low birth weight children. *Pediatrics* **124**, 717–728. https://doi.org/10.1542/peds.2008-2816 (2009).
4. Bhargava, S. K. *et al.* Relation of serial changes in childhood body-mass index to impaired glucose tolerance in young adulthood. *N. Engl. J. Med.* **350**, 865–875. https://doi.org/10.1056/NEJMoa035698 (2004).
5. Hofman, P. L. *et al.* Premature birth and later insulin resistance. *N. Engl. J. Med.* **351**, 2179–2186. https://doi.org/10.1056/NEJMoa042275 (2004).
6. Irving, R. J., Belton, N. R., Elton, R. A. & Walker, B. R. Adult cardiovascular risk factors in premature babies. *Lancet (London, England)* **355**, 2135–2136. https://doi.org/10.1016/s0140-6736(00)02384-9 (2000).
7. Roseboom, T. J. *et al.* Effects of prenatal exposure to the Dutch famine on adult disease in later life: an overview. *Mol. Cell. Endocrinol.* **185**, 93–98. https://doi.org/10.1016/s0303-7207(01)00721-3 (2001).
8. de Rooij, S. R., Wouters, H., Yonker, J. E., Painter, R. C. & Roseboom, T. J. Prenatal undernutrition and cognitive function in late adulthood. *Proc. Natl. Acad. Sci. U.S.A.* **107**, 16881–16886. https://doi.org/10.1073/pnas.1009459107 (2010).
9. Painter, R. C. *et al.* Blood pressure response to psychological stressors in adults after prenatal exposure to the Dutch famine. *J. Hypertens.* **24**, 1771–1778. https://doi.org/10.1097/01.hjh.0000242401.45591.e7 (2006).
10. Gluckman, P. D. & Hanson, M. A. Developmental origins of disease paradigm: a mechanistic and evolutionary perspective. *Pediatr. Res.* **56**, 311–317. https://doi.org/10.1203/01.pdr.0000135998.08025.fb (2004).
11. Gluckman, P. D., Hanson, M. A., Cooper, C. & Thornburg, K. L. Effect of in utero and early-life conditions on adult health and disease. *N. Engl. J. Med.* **359**, 61–73. https://doi.org/10.1056/NEJMra0708473 (2008).
12. Bateson, P. *et al.* Developmental plasticity and human health. *Nature* **430**, 419–421. https://doi.org/10.1038/nature02725 (2004).
13. Schroeder, J. W. *et al.* Neonatal DNA methylation patterns associate with gestational age. *Epigenetics* **6**, 1498–1504. https://doi.org/10.4161/epi.6.12.18296 (2011).
14. Parets, S. E. *et al.* Fetal DNA methylation associates with early spontaneous preterm birth and gestational age. *PLoS ONE* **8**, e67489. https://doi.org/10.1371/journal.pone.0067489 (2013).
15. Simpkin, A. J. *et al.* Longitudinal analysis of DNA methylation associated with birth weight and gestational age. *Hum. Mol. Genet.* **24**, 3752–3763. https://doi.org/10.1093/hmg/ddv119 (2015).
16. Knight, A. K. *et al.* An epigenetic clock for gestational age at birth based on blood methylation data. *Genome Biol.* **17**, 206 (2016).
17. Bohlin, J. *et al.* Prediction of gestational age based on genome-wide differentially methylated regions. *Genome Biol.* **17**, 207. https://doi.org/10.1186/s13059-016-1063-4 (2016).
18. Engel, S. M. *et al.* Neonatal genome-wide methylation patterns in relation to birth weight in the Norwegian Mother and Child Cohort. *Am. J. Epidemiol.* **179**, 834–842. https://doi.org/10.1093/aje/kwt433 (2014).
19. Agha, G. *et al.* Birth weight-for-gestational age is associated with DNA methylation at birth and in childhood. *Clin. Epigenet.* **8**, 118. https://doi.org/10.1186/s13148-016-0285-3 (2016).
20. Cruickshank, M. N. *et al.* Analysis of epigenetic changes in survivors of preterm birth reveals the effect of gestational age and evidence for a long term legacy. *Genome Med.* **5**, 96. https://doi.org/10.1186/gm500 (2013).
21. Benjamini, Y. & Hochberg, Y. Controlling the false discovery rate: a practical and powerful approach to multiple testing. *J. R. Stat. Soc. Ser. B (Methodological)* **57**, 289–300 (1995).
22. Joubert, B. R. *et al.* Maternal plasma folate impacts differential DNA methylation in an epigenome-wide meta-analysis of newborns. *Nat. Commun.* **7**, 10577. https://doi.org/10.1038/ncomms10577 (2016).
23. da Huang, W., Sherman, B. T. & Lempicki, R. A. Systematic and integrative analysis of large gene lists using DAVID bioinformatics resources. *Nat. Protoc.* **4**, 44–57. https://doi.org/10.1038/nprot.2008.211 (2009).
24. Farlik, M. *et al.* DNA methylation dynamics of human hematopoietic stem cell differentiation. *Cell Stem Cell* **19**, 808–822. https://doi.org/10.1016/j.stem.2016.10.019 (2016).
25. Ernst, J. & Kellis, M. Large-scale imputation of epigenomic datasets for systematic annotation of diverse human tissues. *Nat. Biotechnol.* **33**, 364–376. https://doi.org/10.1038/nbt.3157 (2015).
26. Horvath, S. *et al.* An epigenetic clock analysis of race/ethnicity, sex, and coronary heart disease. *Genome Biol.* **17**, 171. https://doi.org/10.1186/s13059-016-1030-0 (2016).
27. Melby, M. K., Yamada, G. & Surkan, P. J. Inadequate gestational weight gain increases risk of small-for-gestational-age term birth in girls in Japan: A population-based cohort study. *Am. J. Hum. Biol.* **28**, 714–720. https://doi.org/10.1002/ajhb.22855 (2016).
28. Moarii, M., Boeva, V., Vert, J. P. & Reyal, F. Changes in correlation between promoter methylation and gene expression in cancer. *BMC Genom.* **16**, 873. https://doi.org/10.1186/s12864-015-1994-2 (2015).
29. Yan, H. *et al.* DNA methylation reactivates GAD1 expression in cancer by preventing CTCF-mediated polycomb repressive complex 2 recruitment. *Oncogene* **35**, 3995–4008. https://doi.org/10.1038/onc.2015.423 (2016).
30. Bonder, M. J. *et al.* Disease variants alter transcription factor levels and methylation of their binding sites. *Nat. Genet.* **49**, 131–138. https://doi.org/10.1038/ng.3721 (2017).
31. Jadhav, U. *et al.* Acquired tissue-specific promoter bivalency is a basis for PRC2 necessity in adult cells. *Cell* **165**, 1389–1400. https://doi.org/10.1016/j.cell.2016.04.031 (2016).
32. Iwasaki, M. & Paszkowski, J. Epigenetic memory in plants. *EMBO J.* **33**, 1987–1998. https://doi.org/10.15252/embj.201488883 (2014).
33. Dean, C. What holds epigenetic memory?. *Nat. Rev. Mol. Cell Biol.* **18**, 140. https://doi.org/10.1038/nrm.2017.15 (2017).
34. Walczewska, J., Dzieza-Grudnik, A., Siga, O. & Grodzicki, T. The role of urocortins in the cardiovascular system. *J. Physiol. Pharmacol* **65**, 753–766 (2014).
35. Diaz, I. *et al.* miR-125a, miR-139 and miR-324 contribute to Urocortin protection against myocardial ischemia-reperfusion injury. *Sci. Rep.* **7**, 8898. https://doi.org/10.1038/s41598-017-09198-x (2017).
36. Demicheva, E. *et al.* Targeting repulsive guidance molecule A to promote regeneration and neuroprotection in multiple sclerosis. *Cell Rep.* **10**, 1887–1898. https://doi.org/10.1016/j.celrep.2015.02.048 (2015).
37. Xiao, B. *et al.* Identification of methylation sites and signature genes with prognostic value for luminal breast cancer. *BMC Cancer* **18**, 405. https://doi.org/10.1186/s12885-018-4314-9 (2018).

38. Korner, A. *et al.* Sympathetic nervous system controls resolution of inflammation via regulation of repulsive guidance molecule A. *Nat. Commun.* **10**, 633. https://doi.org/10.1038/s41467-019-08328-5 (2019).
39. Lee, H. *et al.* DNA methylation shows genome-wide association of NFIX, RAPGEF2 and MSRB3 with gestational age at birth. *Int. J. Epidemiol.* **41**, 188–199. https://doi.org/10.1093/ije/dyr237 (2012).
40. Assenov, Y. *et al.* Comprehensive analysis of DNA methylation data with RnBeads. *Nat. Methods* **11**, 1138–1140. https://doi.org/10.1038/nmeth.3115 (2014).
41. Aryee, M. J. *et al.* Minfi: a flexible and comprehensive Bioconductor package for the analysis of Infinium DNA methylation microarrays. *Bioinformatics (Oxford, England)* **30**, 1363–1369. https://doi.org/10.1093/bioinformatics/btu049 (2014).
42. Morris, T. J. *et al.* ChAMP: 450k chip analysis methylation pipeline. *Bioinformatics (Oxford, England)* **30**, 428–430. https://doi.org/10.1093/bioinformatics/btt684 (2014).
43. Nordlund, J. *et al.* Genome-wide signatures of differential DNA methylation in pediatric acute lymphoblastic leukemia. *Genome Biol.* **14**, r105. https://doi.org/10.1186/gb-2013-14-9-r105 (2013).
44. Chen, Y. A. *et al.* Discovery of cross-reactive probes and polymorphic CpGs in the Illumina Infinium HumanMethylation450 microarray. *Epigenetics* **8**, 203–209. https://doi.org/10.4161/epi.23470 (2013).
45. Triche, T. J. Jr., Weisenberger, D. J., Van Den Berg, D., Laird, P. W. & Siegmund, K. D. Low-level processing of Illumina Infinium DNA Methylation BeadArrays. *Nucleic Acids Res.* **41**, e90. https://doi.org/10.1093/nar/gkt090 (2013).
46. Teschendorff, A. E. *et al.* A beta-mixture quantile normalization method for correcting probe design bias in Illumina Infinium 450 k DNA methylation data. *Bioinformatics (Oxford, England)* **29**, 189–196. https://doi.org/10.1093/bioinformatics/bts680 (2013).
47. Houseman, E. A. *et al.* DNA methylation arrays as surrogate measures of cell mixture distribution. *BMC Bioinform.* **13**, 86. https://doi.org/10.1186/1471-2105-13-86 (2012).
48. Shiwa, Y. *et al.* Adjustment of cell-type composition minimizes systematic bias in blood DNA methylation profiles derived by DNA collection protocols. *PLoS ONE* **11**, e0147519. https://doi.org/10.1371/journal.pone.0147519 (2016).
49. Bakulski, K. M. *et al.* DNA methylation of cord blood cell types: applications for mixed cell birth studies. *Epigenetics* **11**, 354–362. https://doi.org/10.1080/15592294.2016.1161875 (2016).
50. Gelman, A. Scaling regression inputs by dividing by two standard deviations. *Stat. Med.* **27**, 2865–2873. https://doi.org/10.1002/sim.3107 (2008).
51. Lin, X. *et al.* Developmental pathways to adiposity begin before birth and are influenced by genotype, prenatal environment and epigenome. *BMC Med.* **15**, 50. https://doi.org/10.1186/s12916-017-0800-1 (2017).

Acknowledgements

We gratefully acknowledge the families who participated in this study, and the medical staffs at both the Department of Obstetrics and Gynecology & Pediatrics of The University of Tokyo Hospital and the Department of Obstetrics and Gynecology & Neonatology of Tokyo Metropolitan Bokutoh Hospital. This work was supported by the Clinical Research Program for Child Health and Development from Japan Agency for Medical Research and Development, AMED, under Grant Number JP16gk0110007.

Author contributions

K.Kashima, T.K., Y.S., H.K., S.A., K.Matsubara, A.S., K.N. and K.H. performed methylation analysis. K.Kashima, T.K., K.T., K.Matsumoto, K.N. and K.H. performed gene expression analysis. T.N., T.F., I.O., M.S., H.H. and K.Kugu provided specimens for analysis and were also involved in planning the project. K.Kashima, K.U., A.I. and N.T. analyzed epidemiological data. K.Kashima, T.K., R.N., Y.S., K.U., M.M., K.N., K.H. and N.T. generated figures, tables and supplementary information. K.Kashima, T.K., R.N., K.U., K.N., K.H. and N.T. wrote the manuscript. T.K., K.U., A.S., A.O., M.M., K.N., K.H. and N.T. edited the main text and figures. N.T. led the entire project. All authors reviewed the manuscript.

Competing interests

The authors declare no competing interests.

Additional information

Supplementary Information The online version contains supplementary material available at https://doi.org/10.1038/s41598-021-83016-3.

Correspondence and requests for materials should be addressed to K.K.

Reprints and permissions information is available at www.nature.com/reprints.

Publisher's note Springer Nature remains neutral with regard to jurisdictional claims in published maps and institutional affiliations.